Sciencexpress Report

Discovery of a Large Dust Disk Around the Nearby Star AU Microscopium

Paul Kalas,[1,2]* Michael C. Liu,[3] Brenda C. Matthews[1]

[1]Astronomy Department and Radio Astronomy Laboratory, 601 Campbell Hall, Berkeley, CA 94720, USA. [2]National Science Foundation Center for Adaptive Optics, University of California, Santa Cruz, CA 95064, USA. [3]Institute for Astronomy, 2680 Woodlawn Drive, Honolulu, HI 96822, USA.

*To whom correspondence should be addressed. E-mail: kalas@astro.berkeley.edu

We present the discovery of a circumstellar dust disk surrounding AU Microscopium (AU Mic, GJ 803, HD 197481). This young M star at 10 parsec has the same age and origin as β Pictoris, another nearby star surrounded by a dust disk. The AU Mic disk is detected between 50 AU and 210 AU radius, a region where dust lifetimes exceed the present stellar age. Thus, AU Mic is the nearest star where we directly observe the solid material required forplanet formation. Since 85% of stars are M-type, the AU Mic disk provides new clues on how the majority of planetary systems might form and evolve.

About 15% of nearby main-sequence stars exhibit an excess of far-infrared radiation that points to the existence of circumstellar dust grains (*1*). Dust grains have short lifetimes, and their continued presence implies a source of replenishment. The solar system has a disk-like distribution of dust that is continually replenished by the sublimation of comets and collisions between asteroids. We therefore infer that similar populations of undetected parent bodies produce dusty debris disks around infrared excess stars. Moreover, evidence for planets can be found by matching density variations in debris disks to theoretical models of how planets gravitationally perturb these disks (*2*– *4*). In effect, circumstellar debris disks are a signpost for the existence of exosolar planetary systems.

Direct images of debris disks are rare. Starlight reflecting off of optically thin debris disks is detected at optical and near-infrared wavelengths in only three cases - β Pictoris, HR 4796A and HD 141569 (*5*– *7*). In three more cases - Vega, Fomalhaut, and ε Eridani - debris disk structure is seen only at thermal infrared wavelengths (*8*, *9*). β Pic, HR 4796A and HD 141569 are relatively young (<20 Myr) main sequence stars that have the largest disk masses, and hence represent the more detectable of the debris disk systems.

β Pic has Galactic space motions in common with two M stars, AU Mic and AT Mic, that have ages ~20 Myr (*10*). These stars and β Pic may be co-eval sister stars that have separated in space over time due to the small differences in their space motions. A total of 17 stars may be members of this group with age 8–20 Myr (*11*). AU Mic has significant infrared excess at 60 μm (*12*, *13*) and recent sub-millimeter data reveal the presence of cold (40 K) dust, a total dust mass roughly three times smaller than that of β Pic (Table 1), an absence of molecular gas, and a lack of grains within 17 AU of the star (*14*).

We endeavored to directly image circumstellar dust around AU Mic with an optical stellar coronagraph at the University of Hawaii 2.2-m telescope on Mauna Kea, Hawaii (*15*). The stellar coronagraph (fig. S1) produces artificial eclipses of stars by blocking the light at the focal plane with a circular opaque mask suspended by four wires. Instrumental diffracted light is blocked by a Lyot mask in the pupil plane. The net result is significantly enhanced contrast in the regions surrounding bright stars. The imaging camera behind the coronagraph is a Tek 2048×2048 CCD with a scale of 0.41"/pixel. All our data were obtained through a standard broadband *R* filter (λ_c=647 nm, $\Delta\lambda$ = 125 nm).

We acquired data on 14 and 15 October 2003, with 6.5" and 9.5" diameter occulting spots, respectively. We obtained five 240-s and three 300-s images of AU Mic on the first and second nights, respectively. In addition to AU Mic, we observed five other bright stars to check for spurious features such as diffraction spikes and internal reflections (table S1). A disk-like reflection nebulosity surrounding AU Mic was detected in raw data during both nights of observation and does not match the position angle (PA, measured east from north), width, or morphology of instrumental diffraction spikes. The image quality as measured by the full-width at half-maximum (FWHM) of field stars was ~1.1".

Data reduction followed the standard steps of bias subtraction, flat-fielding and sky-subtraction. We then subtracted the stellar point spread function (PSF) to remove excess stellar light from around the occulting spot. We used the real PSF's from other stars observed throughout each night, as well as artificial PSF's. Artificial PSF subtraction is effective for AU Mic because the circumstellar disk is close to edge-on. We extracted the stellar PSF for each image of AU Mic by sampling the image radially in a direction perpendicular to the PA of the disk. We then fit a polynomial to the data and generated an artificial PSF that is a figure of

rotation of the polynomial. The PSF's were then scaled and registered to each data frame such that subtraction minimized the residual light in directions perpendicular to the disk beyond the edge of the occulting spot. In general, the different PSF subtractions produce comparable results, with minor differences appearing a few pixels beyond the edge of the occulting spot. To evaluate the uncertainties in our final image, we measured disk properties in four different data sets that represent two nights of observation, and each with two different PSF subtraction techniques. The data for β Pic from (*16*) that are discussed below were obtained with the same telescope, coronagraph, and filter, and analyzed using similar techniques.

The reflection nebulosity around AU Mic is consistent with a circumstellar disk seen at a near edge-on viewing geometry (Fig. 1, fig. S2). We detect the disk as far as ~21" (210 AU) from the star (*17*). This sensitivity-limited value is a lower limit to the true disk outer radius. The inner radius of the detected disk is 5" (50 AU) and is mainly limited by the radius of the occulting spot and artifacts of the PSF subtraction. The position angles of the two disk midplanes differ by about 6 ± 3°; PA = 124 ± 2° for the SE side and PA = 310° ± 1° for the NW side. A similar, 1.0°–2.5° offset, called the "wing-tilt asymmetry", was measured for the β Pic midplanes (*16*). A symmetric disk can appear to have a wing-tilt when the disk axis is tilted to the line of sight and the scattering phase function is non-isotropic. A model-dependent relationship between the observed wing-tilt and the intrinsic disk inclination (*16*) suggests that AU Mic disk is inclined 7°–20° from edge-on. On the other hand, the sharp midplane morphology is consistent with model disks that have inclinations no greater than ~5° from edge-on (*18*) (fig. S3). Until higher resolution data are obtained and analyzed, we adopt a disk inclination of ~5° from edge-on.

Power-law fits to the disk midplanes between 6" (60 AU) and 16" (120 AU) radius give indices of -3.6 and -3.9 for the NW and SE extensions, respectively (Fig. 2). These indices are similar to the power-law fits for the NE and SW disk extensions of β Pic (Table 1) (*16*). However, the midplane profiles for β Pic become less steep inward of 100 AU. No such turnover is seen for the AU Mic radial profiles. The NW midplane of AU Mic also shows a significant enhancement in surface brightness ~9" radius from the star (Figs. 1 and 2). This could be due to a background source, but further tests using color, polarization and proper motion information should be evaluated before excluding a physical connection to AU Mic.

The existence of morphologically similar dust disks around AU Mic and β Pic supports the hypothesis that these are sister stars born at the same time and location. However, the two disks are not twins. The total mass of dust estimated from the spectral energy distributions is 3.3 times greater for β Pic relative to AU Mic (Table 1). The relative brightnesses of the two disks in optical data are consistent with this result. To make the comparison, we imagine placing the β Pic dust disk around AU Mic. In Figure 2, we include the midplane surface brightness profile for β Pic using data from (*16*) that is now scaled by factors that account for the AU Mic heliocentric distance and stellar luminosity. We find that if the disk of β Pic surrounded AU Mic it would be about 1.5 mag arcsec^{-2} brighter than what we measure for the AU Mic disk (Fig. 2). This corresponds to a factor of four greater scattering cross section of β Pic grains relative to AU Mic grains. If we assume that the two disks have exactly the same structure, grain properties, and viewing geometry then the AU Mic disk requires a dust mass that is four times smaller than that of β Pic. Future observations of disk properties such as the inclination of AU Mic will elucidate the validity of these assumptions, but this result is consistent with the infrared dust luminosity.

The underlying grain properties are also likely to differ due to the weak radiation environment of an M star relative to an A star. AU Mic is three times less massive than β Pic, and 100 times less luminous (Table 1). For the AU Mic disk, the collision timescale at 100 AU radius is 0.2–1.8 Myr assuming a dust optical depth of $\tau \sim 10^{-3}$ –10^{-4}, respectively (fig. S4). At 200 AU, near the outer boundary of the detected disk, the collision timescale is 0.5–5.0 Myr. Given an age of 8–20 Myr for AU Mic, most disk particles have undergone at least one collision. However, as objects are shattered into smaller pieces, the radiation pressure force around AU Mic is too weak to remove the grains (*19*). They can be removed by the system either by joining together to form larger objects, or by spiraling into the star by Poynting-Robertson (PR) drag. The PR timescales at 100 AU are 0.2–2.0 Gyr for 1–10 μm particles, respectively – many times longer than the age of the system (*1*). For β Pic, on the other hand, grains a few microns and smaller are quickly ejected by radiation pressure and the disk mass diminishes over time (*20*). The AU Mic disk should preserve a larger population of sub-micron sized grains, and the mass of solid objects observed today should approximate the primordial disk mass. In other words, most of the disk seen in our optical scattered light image may consist of primordial solid material.

Within ~50 AU of the star, the timescales for grain removal by collisions and PR drag become significantly shorter than the stellar age. Primordial dust at the inner limit of our images (Figs. 1, 2) has mostly vanished, and the grains observed here, as well as those discovered as close as 17 AU from the star (*14*), must be continually replenished by the collisional erosion of much larger objects such as comets and asteroids. The existence of planetesimals in this region lends plausibility to the argument that the same objects will form planets by accretion. Given that AU Mic is only ~10 Myr old,

we may be able to observe planets that are still in the process of accreting mass, or at least discern disk structure that is sculpted by planet-mass bodies. Because AU Mic is closer to the Sun than β Pic, the 2–30 AU zone where terrestrial and gas giant planets might form can be resolved by current and future instrumentation (fig. S5). Planets around AU Mic may also be detected by indirect methods. The low stellar mass means that the star will display a significant astrometric reflex motion (2 milli-arcsec for a Jupiter-analog). The near edge-on orientation favors planet detection by transits of the stellar photosphere. Finally, if a planet is detected by radial velocity techniques, then the near edge-on orientation gives the planet mass by constraining the sin(*i*) ambiguity intrinsic to these measurements.

References and Notes

1. D. E. Backman, F. Paresce, in *Protostars and Protoplanets III*, E. H. Levy, J. I. Lunine, Eds. (University of Arizona Press, Tucson, 1993), pp. 1253-1304.
2. F. Roques, H. Scholl, B. Sicardy, B. A. Smith, *Icarus* **108**, 37 (1994).
3. J.-C. Liou, H. A. Zook, *Astron. J.* **118**, 580 (1999).
4. L. M. Ozernoy, N. N. Gorkavyi, J. C. Mather, T. A. Taidakova, *Astrophys. J.* **537**, L147 (2000).
5. B. A. Smith, R. J.Terrile, *Science* **226**, 1421 (1984).
6. G. Schneider *et al.*, *Astrophys. J.* **513**, L127 (1999).
7. M. D. Silverstone *et al.*, *Bull. Am. Astron. Soc.* **30**, 1363 (1998).
8. W. S. Holland *et al.*, *Nature* **392**, 788 (1998).
9. J. S. Greaves *et al.*, *Astrophys. J.* **506**, L133 (1998).
10. D. Barrado y Navascues, J. R. Stauffer, I. Song, J.-P. Caillault, *Astrophys. J.* **520**, L123 (1999).
11. B. Zuckerman, I. Song, M. S. Bessell, R. A. Webb, *Astrophys. J.* **562**, L87 (2001).
12. V. Tsikoudi, *Astron. J.* **95**, 1797 (1988).
13. I. Song, A. J. Weinberger, E. E. Becklin, B. Zuckerman, C. Chen, *Astron. J.* **124**, 514 (2002).
14. M. C. Liu, B. C. Matthews, J. P. Williams, P. G. Kalas, *Astrophys. J.*, in press.
15. Materials and methods are available as supporting material on *Science* Online.
16. P. Kalas, D. Jewitt, *Astron. J.* **110**, 794 (1995).
17. To increase the signal-to-noise of the data shown in Fig. 1, we binned the data 3×3 pixels and then smoothed by a Gaussian function with σ = 0.5 pixel. This smoothed image was used to find the maximum outer extent of the disk. All other measurements were made using the unbinned and unsmoothed image shown in Fig. 1.
18. P. Kalas, D. Jewitt, *Astron. J.* **111**, 1347 (1996).
19. R. Saija *et al. Mon. Not. R. Astron. Soc.* **341**, 1239 (2003).
20. P. Artymowicz, *Astrophys. J.* **335**, L79 (1988).
21. M. S. Bessel, F. Castelli, B. Plez, *Astron. Astrophys.* **333**, 231(1998).
22. F. Crifo, A. Vidal-Madjar, R. Lallement, R. Ferlet, M. Gerbaldi, *Astron. Astrophys.* **333**, L29 (1997).
23. J. D. Larwood, P. G. Kalas, *Mon. Not. R. Astron. Soc.* **323**, 402 (2001).
24. W. R. F. Dent, H. J. Walker, W. S. Holland, J. S. Greaves, *Mon. Not. R. Astron. Soc.* **314**, 702 (2000).

25. This work has been supported by the NASA Origins Program under grant NAG5-11769, and the NSF Center for Adaptive Optics, managed by the University of California at Santa Cruz under cooperative agreement No. AST-9876783. BCM acknowledges support from NSF grant #0228963. MCL acknowledges support from a Hubble Postdoctoral Fellowship (NASA Grant HST-HF-01152.01). The authors acknowledge the insightful contributions of two anonymous referees.

Supporting Online Material

www.sciencemag.org/cgi/content/full/1093420/DC1
Materials and Methods
Figs. S1to S5
Table S1
References

7 November 2003; accepted 9 February 2004
Published online 26 February 2004; 10.1126/science.1093420
Include this information when citing this paper.

Fig.1. The disk surrounding AU Mic seen in optical scattered light. North is up, east is left, and each side of this false-color image corresponds to 60 arc seconds. The central dark region is produced by the 9.5 arc second diameter focal plane occulting spot which is suspended by four wires and completely masks our direct view of the star. This image represents 900 seconds total integration in the *R* band and each pixel corresponds to 4 AU at the distance to AU Mic. Residual light evident near the occulting spot edge in the NE-SW direction is attributed to asymmetries in the point-spread function caused by instrumental scattering and atmospheric seeing.

Fig. 2. Midplane surface brightness as a function of radius. The midplane was sampled between 5" and 21" radius along a strip 1.2" wide. We show the mean value from two nights of data with two different PSF subtraction techniques. The error bars represent one standard deviation of a single measurement. We fit the data between 6" and 16" radius with power laws that give indices -3.6 and -3.9 for the NW and SE midplanes of AU Mic, respectively. The radial profile for the NW midplane has a significant brightness enhancement at ~ 9" radius that is either intrinsic to the disk or a background object. We also plot the surface brightness of the β Pic disk from (*16*), but with the surface brightness uniformly 3.0 mag arcsec^{-2} fainter to simulate the existence of β Pic's disk

around AU Mic at 9.9 pc. This scaling takes into account the fact that the absolute *R*-band magnitude of AU Mic is 5.6 mag fainter than β Pic (Table 1), and at a constant angular radius the β Pic disk is roughly a factor of $(d_{AU\ Mic} / d_{\beta Pic})^{-3.6}$ = $(9.9 / 19.3)^{-3.6}$ =11.3 times brighter (i.e. 2.6 mag brighter; see Eqn. 4 in *18*).

Table 1. Star (rows 1–8) and disk (rows 9–13) properties for AU Mic and β Pic. The stellar parameters for AU Mic are derived from data given by (*10*, *13*, *21*). For β Pic's stellar parameters, we use (*22*) and references therein. The β Pic disk *R*-band surface brightness (SB) at 6″ radius is given in (*16*), while its maxiumum extent is given in (*23*).

	AU Mic	β Pic
Spectral Type	M1Ve	A5V
Mass ($M_\odot$)	0.5	1.8
T_{eff}(K)	3600	8200
Luminosity ($L_\odot$)	0.09	8.7
Distance (pc)	9.9	19.3
V (mag)	8.81	3.85
M_V (mag)	8.83	2.42
$V - R$	0.88	0.08
Disk SB (6″)	20.1 ± 0.3	15.4 ± 0.3
SB fall-off*	-3.6 to -3.9	-3.8 to -4.1
Max. Radius (AU)	210	1835
$\tau = L_{disk}/L_{bol}$†	6.7×10^{4}	3×10^{3}
Total Dust Mass (g)‡	6.6×10^{25}	2.2×10^{26}

*Value of exponent for a power-law fit to disk Rband surface brightness fall-off between 6-16" radius. The shallower surface brightness profiles correspond to the NW and NE brightness profiles of AU Mic and β Pic, respectively. The β Pic values are taken from (*16*). †The fractional dust luminosity, assuming an optically thin disk, determined by taking the ratio of excess infrared luminosity to stellar bolometric luminosity. The values are obtained from (*13*) and (*1*) for AU Mic and β Pic, respectively. ‡Dust mass from model fits to the spectral energy distributions taken from (*14*) for AU Mic, and (*24*) for β Pic.

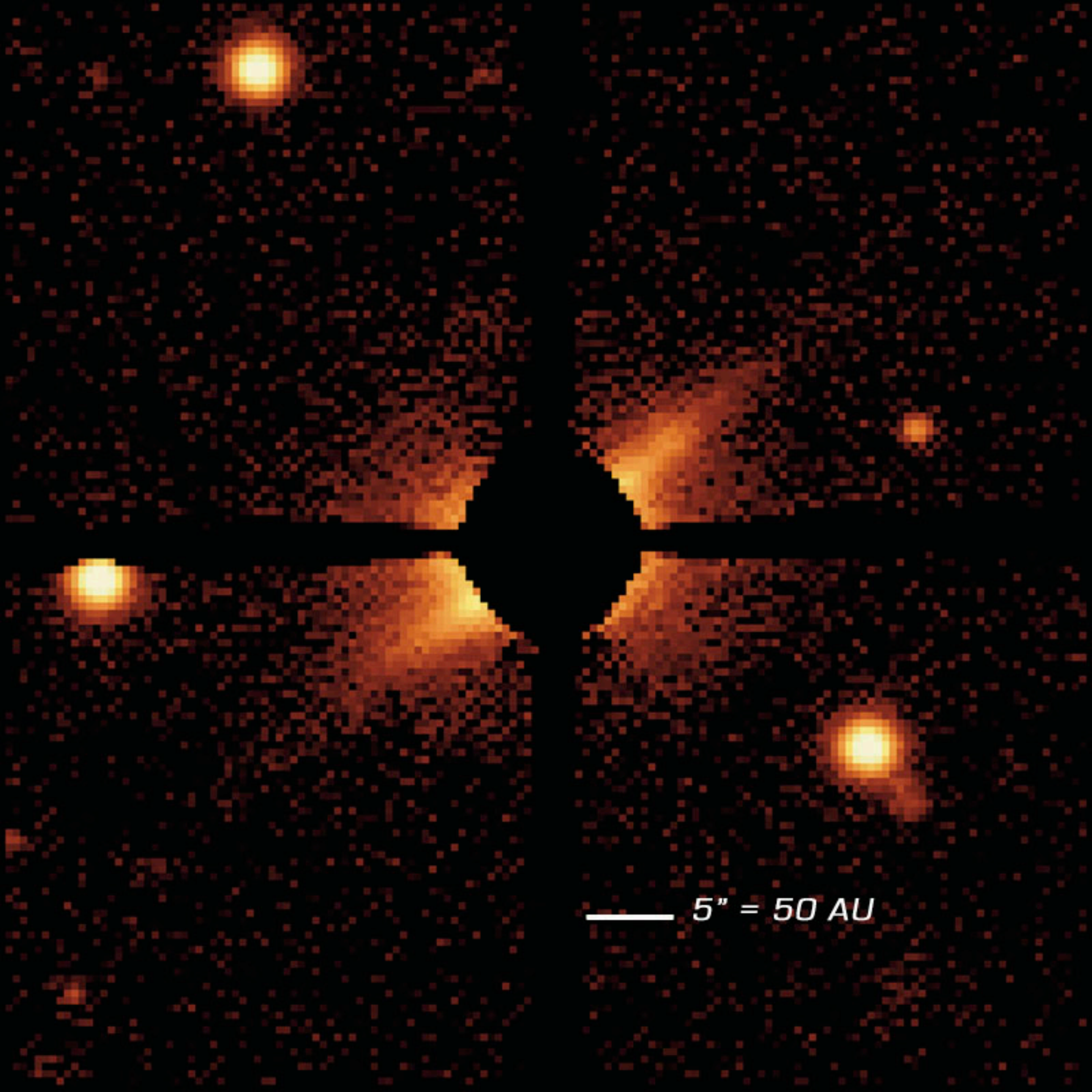
5” = 50 AU

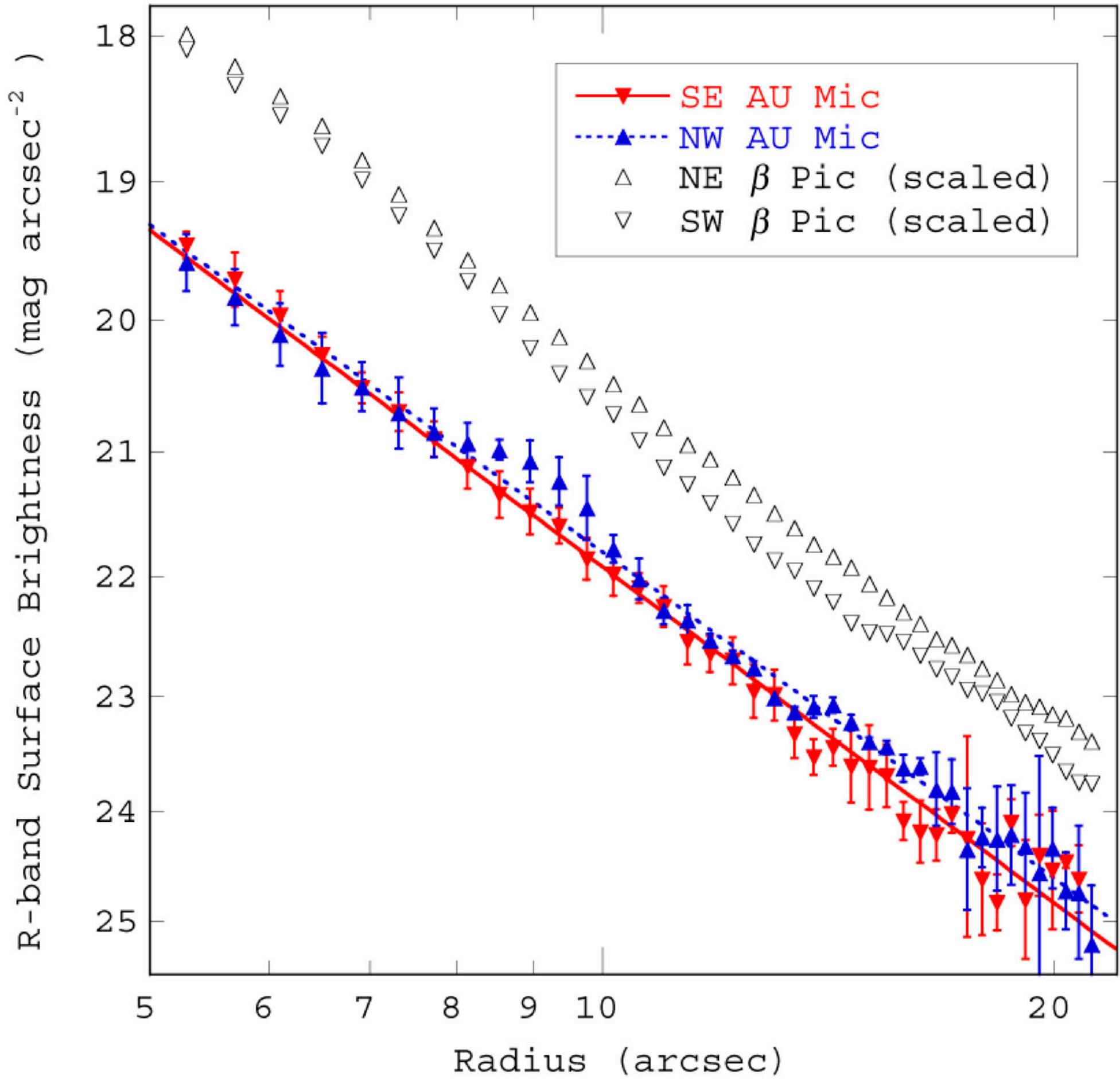
SE AU Mic
NW AU Mic
NE β Pic (scaled)
SW β Pic (scaled)
R-band Surface Brightness (mag arcsec^{-2})
Radius (arcsec)
18
19
20
21
22
23
24
25
5
6
7
8
9
10
20